ISSN 1846-6168 (Print), ISSN 1848-5588 (Online)
https://doi.org/10.31803/tg-20221206210933

Subject review
Received: 2022-12-06, Accepted: 2023-01-12

Comparative Study of Conventional and Microwave-Assisted Boriding of AISI 1040 and AISI 4140 Steels

Safiye İpek Ayvaz, Emre Özer*

Abstract: In this study, AISI 1040 and AISI 4140 steels were boriding using Ekabor-II commercial boriding powder with powder-pack boriding method using microwave and conventional heating methods. The samples were borided at 950 °C for 2 and 6 hours in an Ar atmosphere in a microwave oven of Enerzi-Mh2912-V8. Biphasic structure (FeB/Fe_2B) was formed in all borided AISI 4140 samples and AISI 1040 samples borided for 6 hours. A single-phase structure was observed in AISI 1040 steel borided for 2 hours. Compared to the conventional method, a 1.5-1.6 times thicker boride layer was obtained in AISI 4140 and AISI 1040 steels with microwave-assisted powder-pack boriding. The highest hardness was measured as 1561.8 $HV_{0.05}$ for boriding AISI 4140 steel and 1499.7 $HV_{0.05}$ for boriding AISI 1040 steel. The Vickers indentation fracture toughness of borided steels with microwave energy varied between 2.31 and 3.46 MPa·$m^{1/2}$. It was determined that in all samples borided by the microwave-assisted and conventional powder-pack boriding method, the adhesion strength between the boride layers and the substrate obtained was sufficient.

Keywords: Fe_2B; FeB; fracture toughness; microwave-assisted; powder-pack boriding; steel

1 INTRODUCTION

Boriding is a diffusion-controlled surface hardening process in which boride layers are obtained on the surface by creating a chemical reaction between boron atoms and metal substrate [1, 2]. It is achieved by diffusing boron atoms at high temperatures on the metal substrate in order to increase the wear resistance, surface hardness and corrosion resistance [3, 4]. Boriding, mainly applied to steel and iron alloys, can be used for various surface hardening and heat-treated steels, non-ferrous metal alloys such as titanium, cobalt, nickel, and ceramic materials [5]. With boriding, TiB and TiB_2 in Ti and its alloys, CoB and Co_2B in CoCr alloys and NiB, Ni_2B, and Ni_4B_3 borides are formed in Ni alloys [6-10].

In steel and alloys, the boriding process, generally applied in the temperature range of 800-1050 °C for 0.5-10 hours, is carried out in solid powder, liquid, paste and gas environments. As a result, FeB and Fe_2B hard boride layers are obtained [5, 11]. Apart from these methods, ion deposition, physical and chemical vapor deposition (PVD, CVD), plasma paste and laser methods are also used in order to increase the practicality of layer formation with the developing technology, as well as increase the mechanical properties [12-14]. Powder-pack boriding, one of the boriding varieties, is the most preferred method due to its advantages such as easy application, low cost and changeability of the boriding composition compared to other methods.

Diffusion kinetics of boron [15-17], mechanical [18-20], tribological properties [21-23] and corrosion resistance [24, 25] of borided steels have been investigated in the literature. Uslu et al. borided AISI 1040 steel using Ekabor 2 powder at temperatures of 800, 875 and 950 °C for 2, 4, 6 and 8 hours of soaking times. By the boriding process, they obtained boride layers consisting of FeB and Fe_2B phases, with a hardness of approximately 1500 HVN and a thickness of 10-180 μm [26]. Özerkan borided AISI 1040 steel using Ekabor 2 powder at temperatures of 850 and 950 °C for 2, 4 and 6 h of soaking times. In this study, he examined the microstructural and mechanical properties of the boride layers. It was reported that the obtained thicknesses of the boride layers were 123.4 and 156.3 μm, respectively, at 850 and 950 °C [27]. Ulutan et al. borided AISI 4140 steel using Ekabor 2 powder at temperatures of 900, 950, 1000 and 1050 °C for 2, 4 and 6 hours of soaking times. In the study, the microstructural and tribological properties of boride layers were investigated. They reported a 290 μm boride layer consisting of FeB, Fe_2B and CrB phases was obtained [28]. Keddam et al. borided AISI 4140 steel at 850 and 1000 °C for 2, 4, 6 and 8 hours. They examined the diffusion kinetics of the boron. They determined the boron activation energy as 189.24 kJ·mol^{-1} in AISI 41240 steel [29]. Dominguez et al. borided AISI 4140 steel at temperatures of 850, 900, 950 and 1000 °C for 2, 4, 6 and 8 h. In this study, they found the boron activation energy for the Fe_2B phase as 173 kJ·mol^{-1}. Experimentally, the maximum Fe_2B thickness obtained was 127.9 μm in the sample borided at 1000 °C for 8 h [30]. Çalık et al. borided AISI 316, AISI 1040, AISI 1045, and AISI 4140 steels at 937 °C for 4 hours. They compared the mechanical properties of these steels after boriding. They reported the boride layer thickness as 90 μm in AISI 1040 steel and 100 μm in AISI 4140 steel [31].

In this study, microwave energy was performed powder-pack boriding of AISI 1040 and AISI 4140 steels for the first time in the literature. After boriding and thickness measurements were carried out, some mechanical and microstructural properties were investigated.

2 MATERIAL AND METHOD

In this study, the mechanical and microstructural properties of AISI 1040 and AISI 4140 steels, which are pack-borided using conventional and microwave heating, were investigated. AISI 1040 and AISI 4140 samples were cut by a cut-off machine. Before boriding, the surfaces of the cut samples were cleaned in an ultrasonic bath in acetone

before. As the boriding pack, AISI 304L stainless steel boxes of 50 mm inner diameter and 50 mm height were used. Ekabor II boriding powders with 5% B_4C, 5% KBF_4 and 90% SiC were used as boriding powder. Microwave-assisted boriding process was carried out at 950 °C for 2 and 6 hours in an Ar atmosphere in an Enerzi-Mh2912-V8 brand microwave oven with a power of 2.9 kW and a frequency of 2.45 GHz (Fig. 1).

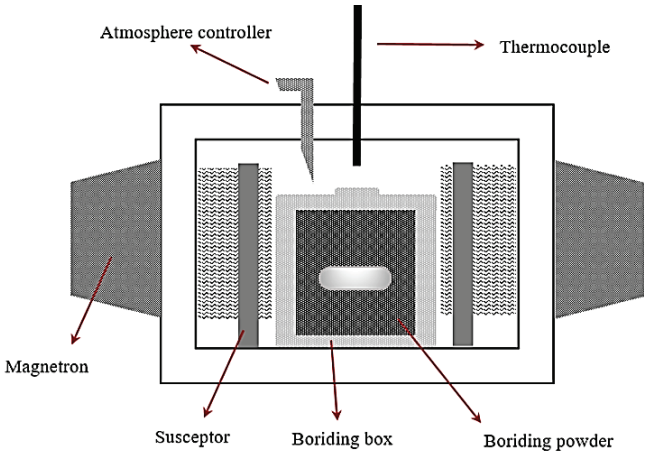

Figure 1 Schematic diagram of the microwave-assisted powder-pack boriding process

After conventional and microwave-assisted boriding, the samples were sanded using 180, 320, 600, 800, 1000 and 1200 grid abrasives and polished using 3 and 1 µm diamond polishing solutions by the Metkon Farcipol 1V brand grinder. After polishing, the samples were etched in a 5% solution of HNO_3 in ethanol (Nital etching reagent). Boride layer thicknesses of etched samples were measured with Nicon Eclipse LV150N brand optical microscope (OM) and Clemex image analysis system. Measurements were repeated eight times for each sample and the average of these measurements was given. Microhardness measurements of the borided samples were performed using the Future-Tech FM 700 brand microhardness measurement device from the cross-section of the sample. In the measurements, 50 gf was applied at an indenter approach speed of 10 µm/sec for 10 seconds. In this study, the equation used to calculate the fracture toughness is as follows:

$$K_{IC} = 0.016 \cdot \frac{P}{c^{1.5}} \cdot \left(\frac{E}{H}\right)^{0.5} \quad (1)$$

Here, E is the elastic modulus of the layer (kg/mm^2) whose fracture toughness is measured, H is the Vickers hardness (HV), P is the applied load (N) during indentation, and c (mm) is the crack length. SEM image of the mark and crack formed on the sample with the Vickers indentation technique is given in Fig. 2.

The adhesion strength between the substrate material and the boride layer in the borided samples was measured following VDI 3198 indentation test standards with a 120° conical indenter. The adhesion behavior was determined by examining cracks, delaminations and fractures in the craters. Microstructural investigations and determination of the adhesion strength of the boride layer were performed using the ZEISS GeminiSEM 500 model (ZEISS, Oberkochen, Germany) scanning electron microscopy (SEM).

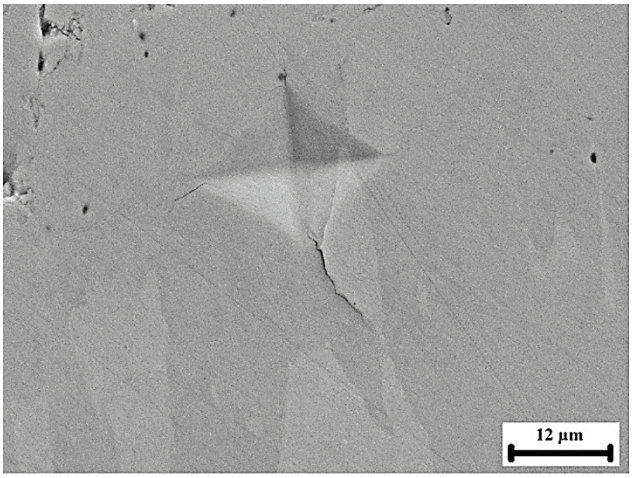

Figure 2 SEM image of the Vickers indentation mark and crack

3 RESULTS AND DISCUSSION

In Figs. 3 and 4, the SEM images of the boride layers of the conventional and microwave-assisted borided samples are given, respectively. While α-Fe has a body-centered cubic structure, neither FeB nor Fe_2B compounds have cubic crystal symmetry [32]. Therefore, B diffusion and boride grain growth exhibit an unnatural anisotropic structure. The preferred growth direction of Fe_2B and FeB compounds is along the 001 direction because B atoms diffuse faster in this direction. As a result, boride grains in the 001 direction perpendicular to the sample surface grow more quickly [20, 33, 34]. Therefore, a boride layer with needle/tooth-like morphology is formed. Saw-tooth morphology also increases the adhesion strength between the substrate and the boride layer [35, 36]. This formation depends on boriding processes such as temperature and time and material properties such as the ratio of the alloy elements [37]. As can be seen in Figs. 3 and 4, boride layers were formed in a saw-tooth form in all samples. As seen in Fig. 3, as the boriding time increased with conventional heating, pores were formed on the surface of the boride layer, especially in AISI 1040 steel. In microwave-assisted boriding, it was determined that both AISI 1040 and AISI 4140 borided steel samples had much less porosity and surface roughness. Therefore a much better surface quality could be obtained with microwave-assisted boriding (Fig. 4).

Due to the high brittleness of the FeB phase, only Fe_2B single-phase structure is preferred after boriding in the steels [38]. Boride layers consisting of the Fe_2B phase were obtained in both AISI 1040 and AISI 4140 steels in the boriding process performed with conventional heating (Figs. 3a-d). Dual-phase structure (dark-colored FeB compound, lighter-colored Fe_2B compound) was observed in microwave-assisted borided AISI 1040 steel for 6 hours (Fig.

4b). A single-phase (Fe_2B) structure was formed in the AISI 1040 steel sample, borided for 2 hours with microwave-assisted heating (Fig. 4a). In AISI 4140 steel, biphasic boride layers were formed as a result of microwave-assisted boriding for both 2 and 6 hours.

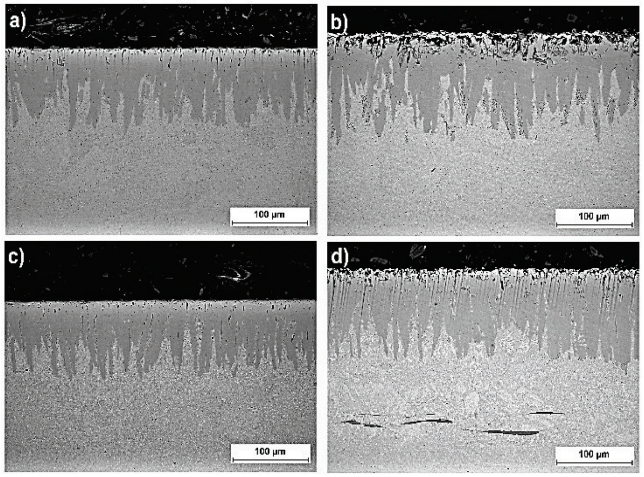

Figure 3 SEM images of the conventional borided samples: a) AISI 1040-2 h, b) AISI 1040-6 h, c) AISI 4140-2 h and d) AISI 4140-6 h

The elemental analysis results obtained from the boride layer and substrate formed in AISI 1040 steel, which was borided for 2 h with conventional heating, are given in Fig. 5. As determined from the EDS analysis, the boride layer was composed of the Fe_2B phase. The change in peak intensity obtained during the linear EDS scanning of B atoms in microwave-assisted borided AISI 4140 for 2 h is seen in Fig. 6. C atoms, like Si atoms, do not dissolve in the boride layer and are pushed toward the substrate during the diffusion of B atoms. In Fig. 6, while C atoms gave a very low peak intensity in the boride layer, it was seen that the peak intensity increased as the scanning went under the layer.

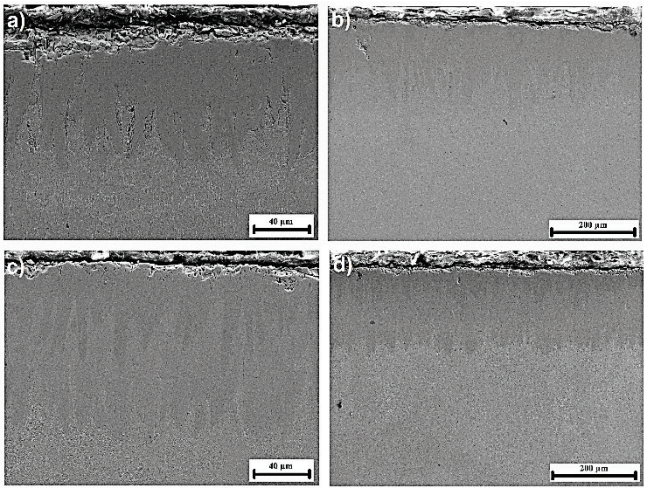

Figure 4 SEM images of the microwave-assisted borided samples: a) AISI 1040-2 h, b) AISI 1040-6 h, c) AISI 4140-2 h and d) AISI 4140-6 h

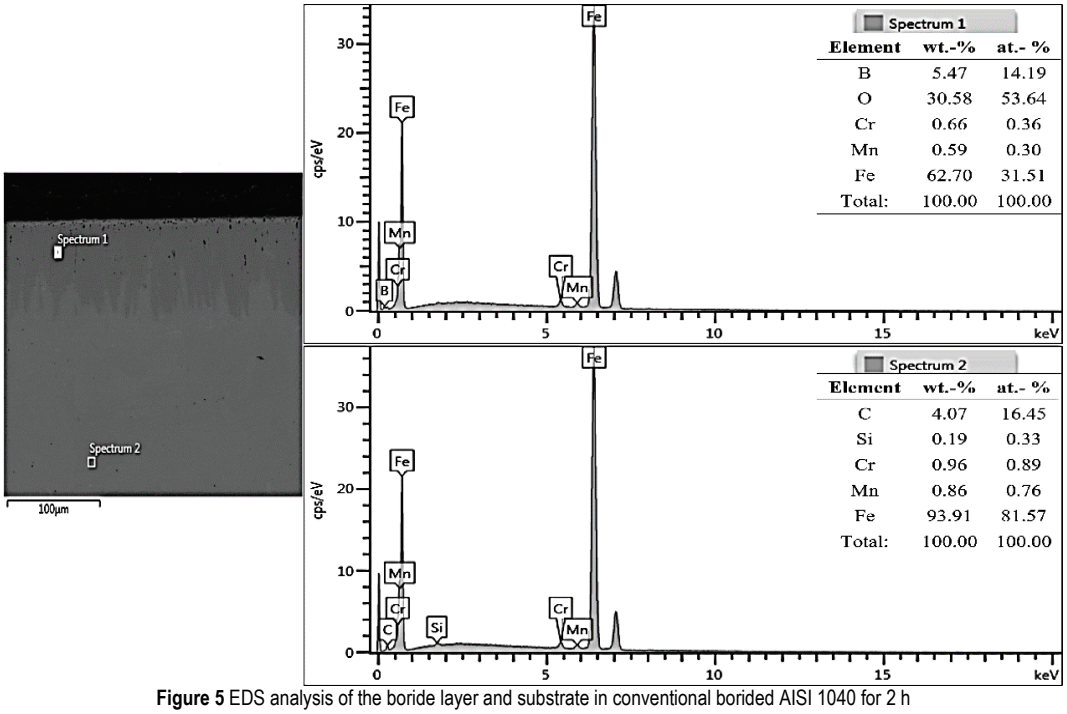

Figure 5 EDS analysis of the boride layer and substrate in conventional borided AISI 1040 for 2 h

Boride layer thicknesses measured in conventional and microwave-assisted powder-pack borided samples are graphically given in Fig. 7. Microwave heating is non-thermal heating. Here, the microwave energy absorbed by the material is transformed into thermal energy [39, 40]. With this energy conversion, rapid volumetric heating occurs. İpek Ayvaz and Aydın [5, 41] borided AISI 316L stainless steel with a microwave-assisted powder-pack boriding method. In this study, two times the thickness of boride was obtained according to the conventional method. In the diffusion kinetics analysis, it was determined that microwave heating increased the pre-exponential factor, and as a result, boron

diffusion increased. When the thickness values obtained in this study are compared with the literature summarized in Tab. 1, it can be seen that the thickness of the boride layer is significantly increased by microwave heating. In particular, the thicknesses obtained in microwave-assisted powder-pack borided AISI 4140 steel are approximately 1.5-2 times the thicknesses in the literature. In this study, it was determined that much thicker boride layers were obtained with microwave-assisted boriding in both AISI 1040 and AISI 4140 steels compared to conventional heating.

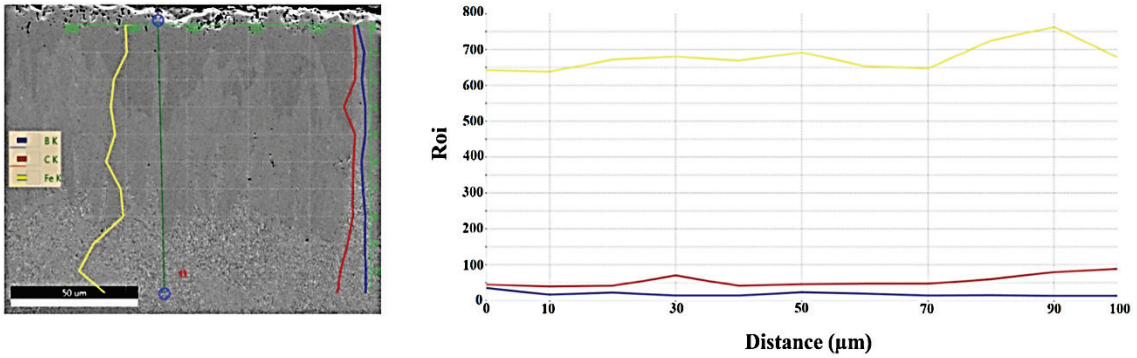

Figure 6 Results of EDS line scan analysis in microwave-assisted borided AISI 4140 for 2 h

Table 1 Boriding parameters applied to AISI 1040 and AISI 4140 steels with a conventional furnace and boriding thicknesses obtained in the literature

Material	Temperature (°C) / Time (h)	Thickness (µm)	References
1040	937 / 4	90-100	[18, 19]
4140	950 / 2	86	[28]
4140	950 / 6	167	[28]
4140	937 / 4	100	[31]
1040	937 / 4	90	[31]
4140	950 / 2	67	[42]
4140	950 / 3	92	[42]
4140	950 / 4	60	[43]
4140	950 / 6	80	[43]

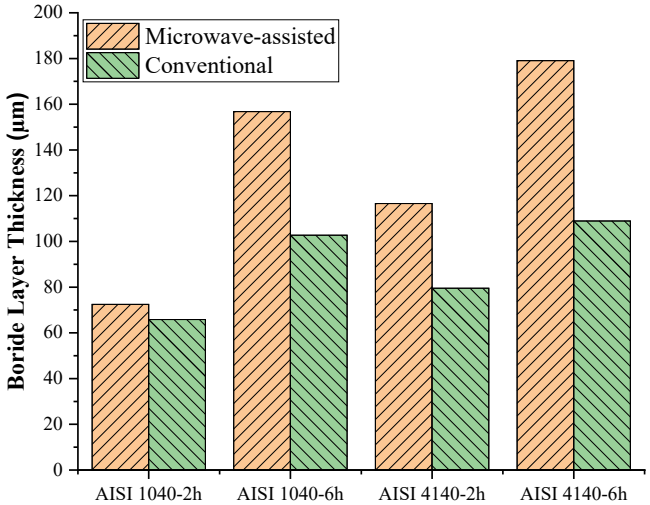

Figure 7 The thickness of boride layers of the conventional and microwave-assisted borided samples

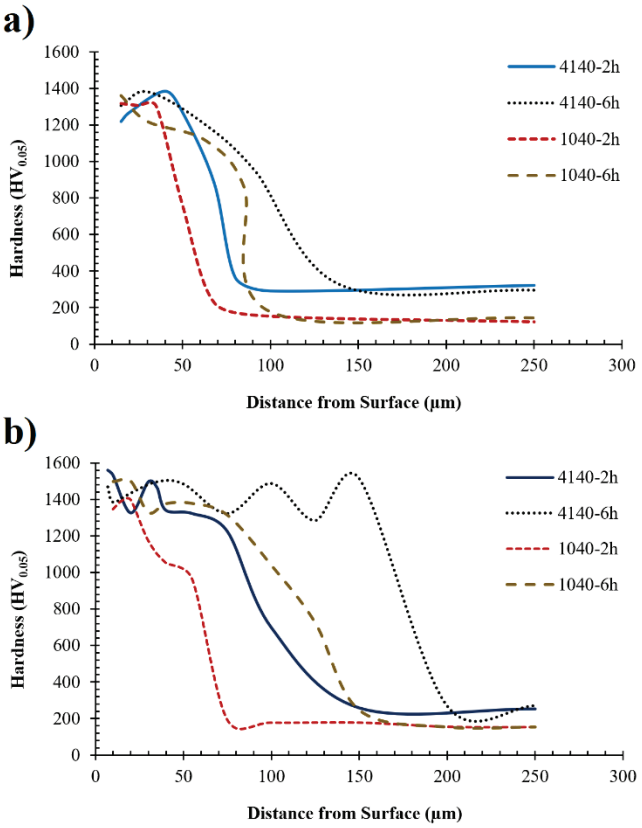

Figure 8 Variation in microhardness as a function of depth from the surface in borided samples a) conventional and b) microwave-assisted

Fig. 8 shows thickness-dependent hardness variations of microwave-assisted and conventional powder-pack borided AISI 4140 and AISI 1040 steels. After the boriding process was performed with the traditional method, the formation of a single-phase Fe_2B layer was detected. With the effect of single-phase structure, sequentially, the maximum microhardness of 1360 and 1384 $HV_{0.05}$ was obtained in AISI 1040 and AISI 4140 steels borided by conventional methods. Uslu et al. [26] obtained a hardness of 1200-1500 HV in borided AISI 1040 steel. Özerkan [27] measured the maximum hardness of 1539.6 HV in borided AISI 1040 steel. In this study, the highest hardness in AISI 1040 steel was measured as approximately 1499 $HV_{0.05}$ in the 10-20 µm depth range from the surface of the microwave-assisted borided sample for 6 hours. Ulutan et al. [28] measured the hardness of borided AISI 4140 steel in the range of 1309-1757 $HV_{0.05}$. Joshi and Hosmani achieved hardness between

1225-1367 $HV_{0.1}$ [42]. Arslan and Akgül Kayral reported the hardness of AISI 4140 steel, which they borided, in the range of approximately 1200-1400 $HV_{0.05}$ [43]. In this study, the highest hardness was measured as 1561 $HV_{0.05}$ in the microwave-borided AISI 4140 sample for 2 hours, and the maximum was 1497 $HV_{0.05}$ in the microwave borided for 6 hours.

Vickers indentation fracture toughness values of borided samples are shown in Fig. 9. When the results given in Fig. 9 are compared, although the fracture toughness of the boride layer obtained with microwave boriding appears to be lower, the crack formation was not observed in the Fe_2B phase in the microwave-borided samples in the tests performed. For these samples, cracks formed in the FeB phase were included in the calculation. However, cracks in the Fe_2B phase in conventionally borided samples were observed. Campos-Silva et al. calculated the fracture toughness of the Fe_2B phase in AISI 4140 steel as 2.9-4.0 $MPa \cdot m^{1/2}$ [20]. Uslu et al. determined the fracture toughness of the boride layers formed in P20 steel in the range of 2.79-4.79 $MPa \cdot m^{1/2}$ [26]. Taktak reported the fracture toughness of boride layers in AISI 304 stainless steel alloy as 2.45-4.08 $MPa \cdot m^{1/2}$ [44]. Campos-Silva et al. determined the fracture toughness of the FeB-Fe_2B interface as 3.56-4.45 $MPa \cdot m^{1/2}$ [45]. In this study, results compatible with the literature were obtained.

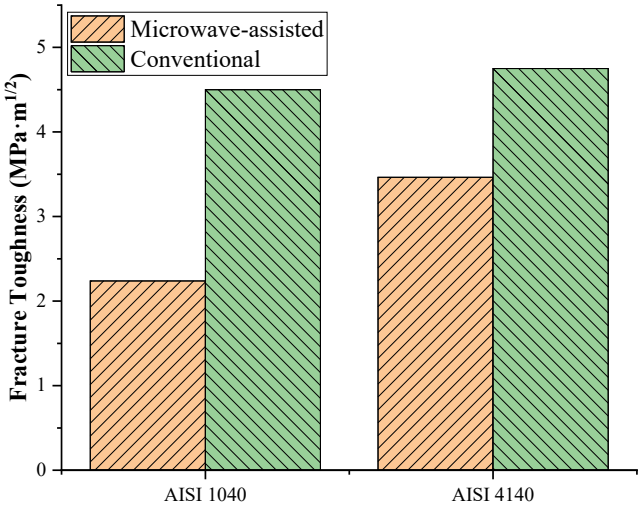

Figure 9 Vickers indentation fracture toughness of the conventional and microwave-assisted borided samples

Figs. 10 and 11 show the SEM images of the craters formed on the surface of the conventional and microwave-assisted borided samples after Daimler-Benz Rockwell-C adhesion tests. Adhesion can be defined as the resistance of a coating to separation or disintegration from the substrate. A standard Rockwell-C hardness tester was used in these tests. In these tests, the damage to the coating was compared with the HF1-HF6 quality map [44, 46, 47], and the adhesion strength between the boride layer and the substrate was evaluated. It is observed that the cratering formed in both microwave-supported and conventionally borided AISI 1040 steels is broader than that of AISI 4140 steel. This situation occurs due to the lower thickness and softer boride layer. This phenomenon can be seen more clearly in microwave-assisted borided samples (Fig. 11). This circumstance was caused by FeB phase formation in microwave-assisted borided AISI 4140 samples. In all samples, sufficient adhesion strength was found between the boride layers and the substrate, meeting the HF1 standard. It is predicted that the increase in the FeB phase may decrease the adhesion strength due to residual thermal stresses [44, 48]. However, it is known that this effect is minimized by hybrid heating that occurs with SiC susceptors in microwave-assisted powder-pack boriding [5, 41].

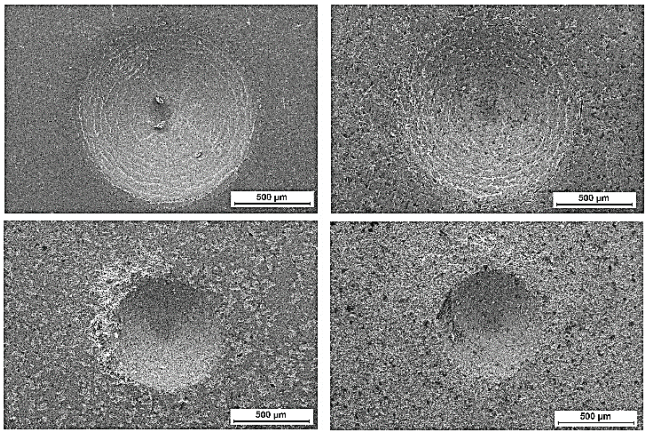

Figure 10 SEM images of craters of the Daimler-Benz adhesion tests on the conventional borided samples: a) AISI 1040-2 h, b) AISI 1040-6 h, c) AISI 4140-2 h and d) AISI 4140-6 h

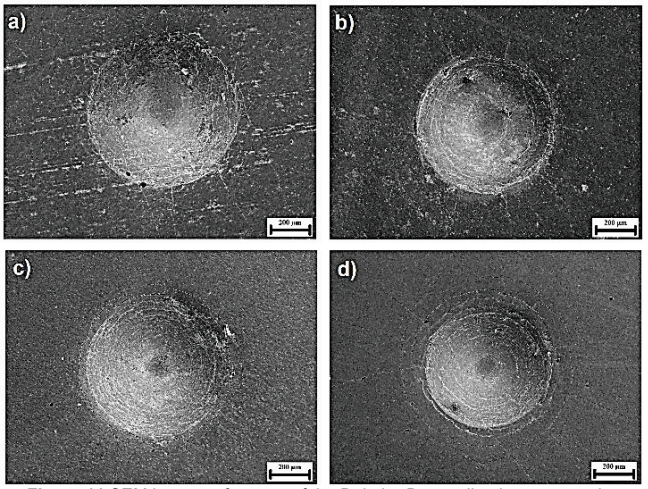

Figure 11 SEM images of craters of the Daimler-Benz adhesion tests on the microwave-assisted borided samples: a) AISI 1040-2 h, b) AISI 1040-6 h, c) AISI 4140-2 h and d) AISI 4140-6 h

4 CONCLUSION

In this study, conventional and microwave-assisted boriding in steel alloys was compared for the first time in the literature. AISI 4140 and AISI 1040 steels were borided using microwave-assisted and conventional powder pack boriding methods. The results obtained after the boriding process was applied at 950 °C for 2 and 6 hours are as follows:

- While a single-phase (Fe_2B) boride layer was observed in all conventional borided samples, a single-phase boride layer was obtained in AISI 1040 steel borided for only 2 hours from microwave-assisted borided samples. In other samples, FeB/Fe_2B biphasic boride layers were formed.
- Boride layer thicknesses were approximately 1.5-2 times thicker than the literature obtained in AISI 4140 steel due to microwave-assisted boriding. These thicknesses were 116.6 and 179.01 μm after boring for 2 and 6 hours, respectively. With microwave-assisted boriding, a ~60% increase in thickness was achieved compared to the conventional method.
- Boride layer thicknesses of 72.48 and 156.8 μm were obtained in AISI 1040 steel, respectively, after 2 and 6 hours of boriding. With microwave-assisted boriding, a ~50% increase in thickness was achieved compared to the conventional method.
- The highest hardnesses obtained in microwave-assisted borided AISI 4140 and AISI 1040 steels are 1561.8 $HV_{0.05}$ and 1499.7 $HV_{0.05}$, respectively.
- According to the results in the literature, fracture toughness was calculated between 2.31 and 3.46 $MPa \cdot m^{1/2}$ in microwave energy borided samples. The fracture toughness of the boride layers in the conventionally borided samples with a boride layer consisting of a single-phase Fe_2B compound is higher than in the microwave-assisted borided ones.
- It was determined that there was sufficient adhesion strength between the boride layers and the substrate in all samples.

5 REFERENCES

[1] Ozdemir, O., Omar, M. A., Usta, M., Zeytin, S., Bindal, C., & Ucisik, A. H. (2009). An investigation on boriding kinetics of AISI 316 stainless steel. *Vacuum*, *83*(1), 175-179. https://doi.org/10.1016/j.vacuum.2008.03.026

[2] Genel, K. (2006). Boriding kinetics of H13 steel. *Vacuum*, *80*(5), 451-457. https://doi.org/10.1016/j.vacuum.2005.07.013

[3] Abdellah, Z. N., Boumaali, B., & Keddam, M. (2021). Experimental evaluation and modelling of the boronizing kinetics of AISI H13 hot work tool steel. *Materials Testing*, *63*(12), 1136-1141. https://doi.org/10.1515/mt-2021-0056

[4] Yu, L. G., Chen, X. J., Khor, K. A., & Sundararajan, G. (2005). FeB/Fe_2B phase transformation during SPS pack-boriding: Boride layer growth kinetics. *Acta Materialia*, *53*(8), 2361-2368. https://doi.org/10.1016/j.actamat.2005.01.043

[5] Ayvaz, S. İ. & Aydın, İ. (2020). Effect of the microwave heating on diffusion kinetics and mechanical properties of borides in AISI 316L. *Transactions of the Indian Institute of Metals*, *73*(10), 2635-2644. https://doi.org/10.1007/s12666-020-02072-x

[6] Boumaali, B., Abdellah, Z. N., & Keddam, M. (2021). Computer simulation of boronizing kinetics for a TB_2 alloy. *Materials Testing*, *63*(12), 1130-1135. https://doi.org/10.1515/mt-2021-0051

[7] Deng, D., Wang, C., Liu, Q., & Niu, T. (2015). Effect of standard heat treatment on microstructure and properties of borided Inconel 718. *Transactions of Nonferrous Metals Society of China*, *25*(2), 437-443. https://doi.org/10.1016/S1003-6326(15)63621-4

[8] Makuch, N., Kulka, M., Keddam, M., Taktak, S., Ataibis, V., & Dziarski, P. (2017). Growth kinetics and some mechanical properties of two-phase boride layers produced on commercially pure titanium during plasma paste boriding. *Thin Solid Film*, *626*, 25-37. https://doi.org/10.1016/j.tsf.2017.02.033

[9] Tsipas, S. A., Vázquez-Alcázar, M. R., Navas, E. M. R., & Gordo, E. (2010). Boride coatings obtained by pack cementation deposited on powder metallurgy and wrought Ti and Ti–6Al–4V. *Surface and Coatings Technology*, *205*(7), 2340-2347. https://doi.org/10.1016/j.surfcoat.2010.09.026

[10] Campos-Silva, I., Bravo-Bárcenas, D., Cimenoglu, H., Figueroa-López, U., Flores-Jiménez, M., & Meydanoglu, O. (2014). The boriding process in CoCrMo alloy: Fracture toughness in cobalt boride coatings. *Surface and Coatings Technology*, *260*, 362-368. https://doi.org/10.1016/j.surfcoat.2014.07.092

[11] Sen, S., Sen, U., & Bindal, C. (2006). Tribological properties of oxidised boride coatings grown on AISI 4140 steel. *Materials Letters*, *60*(29–30), 3481-3486. https://doi.org/10.1016/j.matlet.2006.03.036

[12] Çelikkan, H., Öztürk, M. K., Aydin, H., & Aksu, M. L. (2007). Boriding titanium alloys at lower temperatures using electrochemical methods. *Thin Solid Films*, *515*(13), 5348-5352. https://doi.org/10.1016/j.tsf.2007.01.020

[13] Yoon, J. H., Jee, Y. K., & Lee, S. Y. (1999). Plasma paste boronizing treatment of the stainless steel AISI 304. *Surface and Coatings Technology*, *112*(1-3), 71-75. https://doi.org/10.1016/S0257-8972(98)00743-9

[14] Selvan, J. S., Subramanian, K., Nath, A. K., Kumar, H., Ramachandra, C., & Ravindranathan, S. P. (1999). Laser boronising of Ti–6Al–4V as a result of laser alloying with pre-placed BN. *Materials Science and Engineering: A*, *260*(1-2), 178-187. https://doi.org/10.1016/S0921-5093(98)00964-2

[15] Genel, K., Ozbek, I., & Bindal, C. (2003). Kinetics of boriding of AISI W1 steel. *Materials Science and Engineering: A*, *347*(1-2), 311-314. https://doi.org/10.1016/S0921-5093(02)00607-X

[16] Bektes, M., Calik, A., Ucar, N., & Keddam, M. (2010). Pack-boriding of Fe–Mn binary alloys: Characterization and kinetics of the boride layers. *Materials Characterization*, *61*(2), 233-239. https://doi.org/10.1016/j.matchar.2009.12.005

[17] Ucar, N., Yigit, M., & Calik, A. (2020). Metallurgical characterization and kinetics of borided 34CrNiMo6 steel. *Advances in Materials Science*, *20*(4), 38-48. https://doi.org/10.2478/adms-2020-0021

[18] Calik, A., Sahin, O., & Ucar, N. (2008). Specimen geometry effect on the mechanical properties of AISI 1040 steel. *Zeitschrift für Naturforschung A*, *63*(7-8), 448-452. https://doi.org/10.1515/zna-2008-7-811

[19] Calik, A., Taylan, F., Sahin, O., & Ucar, N. (2009). Comparison of mechanical properties of boronized and vanadium carbide coated AISI 1040 steels. *Indian Journal of Engineering and Materials Sciences*, *16*(5), 326-330.

[20] Campos-Silva, I., Ortiz-Domínguez, M., López-Perrusquia, N., Meneses-Amador, A., Escobar-Galindo, R., & Martinez-Trinidad, J. (2010). Characterization of AISI 4140 borided steels. *Applied Surface Science*, *256*(8), 2372-2379. https://doi.org/10.1016/j.apsusc.2009.10.070

[21] Fernández-Valdés, D., Meneses-Amador, A., López-Liévano, A., & Ocampo-Ramírez, A. (2021). Sliding wear analysis in borided AISI 316L steels. *Materials Letters*, *285*, 129138. https://doi.org/10.1016/j.matlet.2020.129138

[22] García-Léon, R. A., Martínez-Trinidad, J., Campos-Silva, I., Figueroa-López, U., & Guevara-Morales, A. (2021). Wear maps of borided AISI 316L steel under ball-on-flat dry sliding conditions. *Materials Letters*, *282*, 128842. https://doi.org/10.1016/j.matlet.2020.128842

[23] Ficici, F., Kapsiz, M., & Durat, M. (2011). Applications of taguchi design method to study wear behaviour of boronized AISI 1040 steel. *International Journal of the Physical Sciences*, *6*(2), 237-243. https://doi.org/10.5897/IJPS11.009

[24] da Costa Aichholz, S. A., Meruvia, M. S., Júnior, P. C. S., & Torres, R. D. (2018). Tribocorrosion behavior of boronized AISI 4140 steel. *Surface and Coatings Technology*, *352*, 265-272. https://doi.org/10.1016/j.surfcoat.2018.07.101

[25] D'Souza, B., Leong, A., Yang, Q., & Zhang, J. (2021). Corrosion behavior of boronized nickel-based alloys in the molten chloride Salt. *Corrosion Science*, *182*, 109285. https://doi.org/10.1016/j.corsci.2021.109285

[26] Uslu, I., Comert, H., Ipek, M., Celebi, F. G., Ozdemir, O., & Bindal, C. (2007). A comparison of borides formed on AISI 1040 and AISI P20 steels. *Materials and Design*, *28*(6), 1819-1826. https://doi.org/10.1016/j.matdes.2006.04.019

[27] Özerkan, H. B. (2019). Experimental fatigue life determination of thermo-diffusion surface boronized of AISI 1040 steel. *Journal of Mechanical Science and Technology*, *33*(10), 4957-4962. https://doi.org/10.1007/s12206-019-0935-4

[28] Ulutan, M., Yildirim, M. M., Çelik, O. N., & Buytoz, S. (2010). Tribological properties of borided AISI 4140 steel with the powder pack-boriding method. *Tribology Letters*, *38*(3), 231-239. https://doi.org/10.1007/s11249-010-9597-1

[29] Keddam, M., Ortiz-Domínguez, M., Gómez-Vargas, O. A., Arenas-Flores, A., Flores-Rentería, M. Á., Elias-Espinosa, M., & García-Barrientos, A. (2015). Kinetic study and characterization of borided AISI 4140 steel. *Materiali in Tehnologije - Materials and Technology*, *49*(5), 665-672. https://doi.org/10.17222/mit.2014.034

[30] Ortiz-Domínguez, M., Hernandez-Sanchez, E., Martinez-Trinidad, J., Keddam, M., & Campos-Silva, I. (2010). A kinetic model for analyzing the growth kinetics of Fe_2B layers in AISI 4140 steel. *Kovové Materiály - Metallic Materials*, *48*, 285-290. https://doi.org/10.4149/km_2010_5_285

[31] Calik, A., Sahin, O., & Ucar, N. (2009). Mechanical properties of boronized AISI 316, AISI 1040, AISI 1045 and AISI 4140 steels. *Acta Physica Polonica A*, *115*(3), 694-698. https://doi.org/10.12693/aphyspola.115.694

[32] Pomel'nikova, A. S., Shipko, M. N., & Stepovich, M. A. (2011). Features of structural changes due to the formation of the boride crystal structure in steels. *Journal of Surface Investigation: X-ray, Synchrotron and Neutron Techniques*, *5*(2), 298-304. https://doi.org/10.1134/S1027451011030165

[33] Ramdan, R. D., Takaki, T., Yashiro, K., & Tomita, Y. (2010). The effects of structure orientation on the growth of Fe_2B boride by multi-phase-field simulation. *Materials Transactions*, *51*(1), 62-67. https://doi.org/10.2320/matertrans.M2009227

[34] Brakman, C. M., Gommers, A. W. J., & Mittemeijer, E. J. (1989). Boriding of Fe and Fe–C, Fe–Cr, and Fe–Ni alloys; boride-layer growth kinetics. *Journal of Materials Research*, *4*(6), 1354-1370. https://doi.org/10.1557/JMR.1989.1354

[35] İpek, M., Celebi Efe, G., Ozbek, I., Zeytin, S., & Bindal, C. (2012). Investigation of boronizing kinetics of AISI 51100 steel. *Journal of Materials Engineering and Performance*, *21*(5), 733-738. https://doi.org/10.1007/s11665-012-0192-5

[36] Garcia-Bustos, E., Figueroa-Guadarrama, M. A., Rodriguez-Castro, G. A., Gómez-Vargas, O. A., Gallardo-Hernandez, E. A., & Campos-Silva, I. (2013). The wear resistance of boride layers measured by the four-ball test. *Surface and Coatings Technology*, *215*, 241-246. https://doi.org/10.1016/j.surfcoat.2012.08.090

[37] Ozbek, I. & Bindal, C. (2002). Mechanical properties of boronized AISI W4 steel. *Surface and Coatings Technology*, *154*(1), 14-20. https://doi.org/10.1016/S0257-8972(01)01409-8

[38] Ozdemir, O., Usta, M., Bindal, C., & Ucisik, A. H. (2006). Hard iron boride (Fe_2B) on 99.97 wt% pure iron. *Vacuum*, *80*(11-12), 1391-1395. https://doi.org/10.1016/j.vacuum.2006.01.022

[39] Ayvaz, M. (2022). Characterization and tribological properties of novel AlCu4.5SiMg alloy–(B_4C/TiO_2/nGr) quaternary hybrid composites sintered via microwave. *Metals and Materials International*, *28*, 710-721. https://doi.org/10.1007/s12540-020-00894-4

[40] Ayvaz, M. (2021). Microstructure and dry sliding wear behaviors of microwave-sintered Al-4.4Cu-0.7Mg-0.6Si-B_4C/nGr hybrid composites. *Transactions of the Indian Institute of Metals*, *74*(6), 1397-1408. https://doi.org/10.1007/s12666-021-02232-7

[41] Ayvaz, S. İ. & Aydin, İ. (2022). Tribological and adhesion properties of microwave-assisted borided AISI 316L steel. *Materials Testing*, *64*(2), 249-259. https://doi.org/10.1515/mt-2021-2031

[42] Joshi, A. A. & Hosmani, S. S. (2014). Pack-boronizing of AISI 4140 steel: Boronizing mechanism and the role of container design. *Materials and Manufacturing Processes*, *29*(9), 1062-1072. https://doi.org/10.1080/10426914.2014.921705

[43] Arslan, D. & Akgün, S. (2021). Mechanical characterization of pack-boronized AISI 4140 and AISI H13 steels. *International Advanced Researches and Engineering Journal*, *5*(1), 61-71. https://doi.org/10.35860/iarej.817274

[44] Taktak, S. (2007). Some mechanical properties of borided AISI H13 and 304 steels. *Materials and Design*, *28*(6), 1836-1843. https://doi.org/10.1016/j.matdes.2006.04.017

[45] Campos-Silva, I., Martinez-Trinidad, J., Doñu-Ruíz, M. A., Rodríguez-Castro, G., Hernandez-Sanchez, E., & Bravo-Bárcenas, O. (2011). Interfacial indentation test of FeB/Fe_2B coatings. *Surface and Coatings Technology*, *206*(7), 1809-1815. https://doi.org/10.1016/j.surfcoat.2011.08.017

[46] Vera Cárdenas, E. E., Lewis, R., Martínez Pérez, A. I., Bernal Ponce, J. L., Pérez Pinal, F. J., Domínguez, M. O., & Rivera Arreola, E. D. (2016). Characterization and wear performance of boride phases over tool steel substrates. *Advances in Mechanical Engineering*, *8*(2), 1687814016630257. https://doi.org/10.1177/1687814016630257

[47] Vidakis, N., Antoniadis, A., & Bilalis, N. (2003). The VDI 3198 indentation test evaluation of a reliable qualitative control for layered compounds. *Journal of Materials Processing Technology*, *143-144*, 481-485. https://doi.org/10.1016/S0924-0136(03)00300-5

[48] Krelling, A. P., Da Costa, C. E., Milan, J. C. G., & Almeida, E. A. S. (2017). Micro-abrasive wear mechanisms of borided AISI 1020 steel. *Tribology International*, *111*, 234-242. https://doi.org/10.1016/j.triboint.2017.03.017

Authors' contacts:

Safiye İpek Ayvaz, Lect. Dr.
Celal Bayar University,
Turgutlu Vocational School,
Department of Machinery and Metal Technologies,
45140 Manisa, Turkey
s.ipekayvaz@gmail.com

Emre Özer, Asst. Prof. Dr.
(Corresponding author)
Osmaniye Korkut Ata University,
Engineering Faculty,
Department of Industrial Engineering,
80000 Osmaniye, Turkey
mech.eng.emreozer@gmail.com